

# The Analysis and Design of Single Plate Framing Connections

RALPH M. RICHARD, PAUL E. GILLETT, JAMES D. KRIEGH, AND BRETT A. LEWIS

The single plate framing connection has been considered by designers to be a flexible connection that is economical in both material and fabrication requirements in the erection of steel buildings. Two typical single plate framing connections are shown in Figs. 1 and 2. In both cases, the connection comprises a single plate, with prepunched bolt holes, that is shop welded to the supporting member. During erection, the beam with prepunched holes is brought into position and field bolted to the framing plate.

The standard design procedure for the single plate framing connection is to assume each bolt carries an equal portion of the total shear load and, in agreement with the simple support assumption, that relatively free rotation occurs between the end of the beam and the supporting member. In fact, because of these simplifications the single plate framing connection is often called the "shear tab." Investigations into the structural action, strength, and ductility of the single plate framing connection have been limited<sup>1-3</sup> and none have satisfactorily proved or disproved the validity of the standard design procedure. Even though this connection has an apparent failure-free performance record, this does not necessarily indicate that good design procedures have been used; the actual load and stress distributions should be understood and the design methods and specifications should reflect the actual structural behavior.

---

*Ralph M. Richard is Professor, Dept. of Civil Engineering and Engineering Mechanics, University of Arizona, Tucson, Arizona.*

*Paul E. Gillett is Asst. Professor, Dept. of Civil Engineering, Texas Tech University, Lubbock, Texas.*

*James D. Kriegh is Professor, Dept. of Civil Engineering and Engineering Mechanics, University of Arizona, Tucson, Arizona.*

*Brett A. Lewis is Graduate Assistant, Dept. of Civil Engineering and Engineering Mechanics, University of Arizona, Tucson, Arizona.*

---

*This paper was presented at the AISC National Engineering Conference in Pittsburgh, Pennsylvania on April 30, 1980.*

The single plate framing connection, unlike the framed beam connection, which has elements subjected to flexure to give it ductility, derives its limited ductility from: (1) bolt deformation in shear, (2) plate and/or beam web hole distortion, and (3) out-of-plane bending of the plate and/or beam web. Additional ductility may occur from bolt slippage if the bolts are not in bearing at the time of initial loading. Tests and studies reported herein as well as by Lipson<sup>1,2</sup> indicate that the single plate connection can develop a significant end moment in the beam and supporting member. The magnitude of the moment is generally dependent upon: (1) the number, size, and configuration of

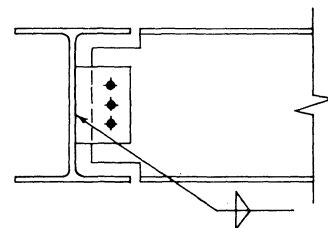


Fig. 1. Single plate framing connection connecting beam to web of supporting beam

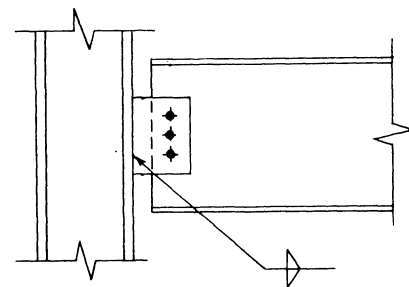


Fig. 2. Single plate framing connection connecting beam to flange of supporting column

bolt pattern, (2) the thickness of the plate and/or beam web, (3) the beam span to beam depth ratio, (4) the loading (whether uniform or concentrated), and (5) the relative flexibility of the supporting structural element, such as a column or a girder, as shown in Figs. 1 and 2. Therefore, before the connection moment can be determined, all the connection variables listed above must be considered. However, it is beyond the scope of this research effort to include the relative flexibility of the beam and connection to the supporting structure. It is noted that for one-sided connections, such as shown in Figs. 1 and 2, the flexibility of the supporting elements can very significantly reduce the connection moment. When the connection is used on both sides of a supporting structure with resulting symmetry, however, the connection may be considered attached to a rigid support. This latter case of full restraint at the welded edge of the plate was assumed in the analytical models and approximated in the physical tests in the research reported herein.

### METHOD OF ANALYSIS

In order to evaluate the end moment generated by the single plate framing connection, the well-known beam line method<sup>4-6</sup> was used. This method consists of the construction of a "beam line" on a connection moment-rotation curve, as shown in Fig. 3. The vertical axis intercept of the beam line is the beam fixed end moment, whereas the horizontal axis intercept of this line is the simple span end

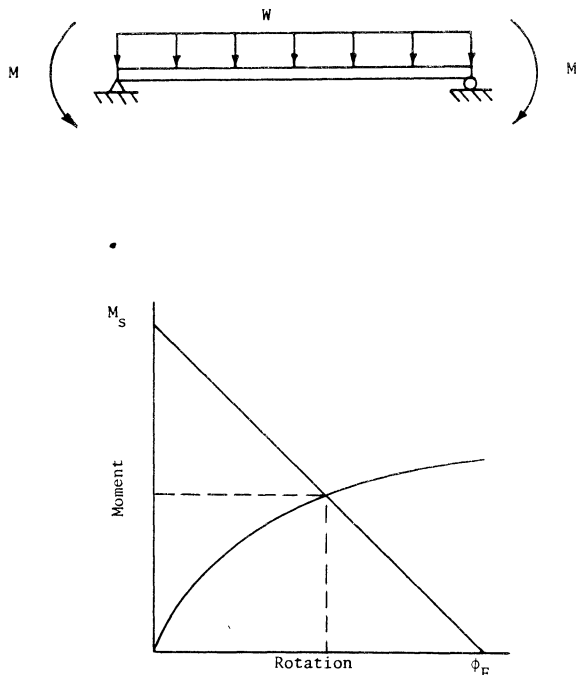


Fig. 3. Moment-rotation relationship

rotation of the beam. The intersection of the beam line and the moment rotation curve for the connection gives the moment and rotation at the end of the beam. This procedure utilizes directly the nonlinear moment-rotation action of the connection and assumes linear action for the beam.

### MOMENT-ROTATION CURVES BASED UPON SINGLE SHEAR BOLT TESTS

The procedure used in establishing moment-rotation curves or single plate framing connection was based upon a nonlinear finite element analysis developed by the senior author and demonstrated by Caccavale.<sup>3</sup> The method consisted of two parts. These are: (a) determining experimentally the load-deformation relationship for a single bolt connecting two plates in single shear, which lumps together all linear and nonlinear deformations occurring in the bolt and the connected plates, and (b) analyzing the connection using the finite element method in which the nonlinear behavior of the bolts and the connected plates was modeled as a shear connector with load-deformation properties obtained from (a).

In order to achieve the objectives of this study, the following steps were followed:

1. A series of single bolt, single shear tests was performed for the range of bolt diameters and plate thicknesses typical of single plate framing connections.
2. Finite element models were developed for a sufficient number of single plate framing connection configurations, in order that trends in behavior could be determined.
3. Moment-rotation curves were obtained through finite element model analyses. This included developing a nondimensional analytical expression capable of representing typical framing plate designs.
4. Full scale laboratory tests were made on two-, three-, five-, and seven-bolt connections to verify the adequacy of the analytical results.

**Single Bolt-Single Shear Tests**—When this study was initiated, the extent of single bolt, single shear load-deformation tests consisted of a limited number of tests performed by Caccavale.<sup>3</sup> Because the double shear tests did not satisfy the modeling requirements, a total of 126 single bolt, single shear load-deformation tests were made.

The testing program included the bolt and plate combinations shown in Table 1. In setting up the testing program, the following limitations were made:

1. Only ASTM A325 and ASTM A490 bolts were used.
2. Bolt diameters were  $\frac{3}{4}$ -in.,  $\frac{7}{8}$ -in., and 1-in.
3. Plate materials were ASTM A36 and ASTM A575 Grade 50 steel. (Although A36 steel was considered as

**Table 1. Test Program for Single Bolt, Single Shear Tests**  
(X denotes at least one test)

Plate Combinations		A325 Bolts			A490 Bolts		
		3/4-in.	7/8-in.	1-in.	3/4-in.	7/8-in.	1-in.
A36	1/4, 1/4	X					
	1/4, 3/8	X	X				
	1/4, 1/2	X	X				
	5/16, 5/16	X	X				
	3/8, 3/8	X	X		X		
	3/8, 1/2	X	X				
	7/16, 7/16	X	X		X	X	
	1/2, 1/2	X	X	X	X	X	X
A572 Gr 50	3/8, 3/8	X	X		X	X	
	1/2, 1/2				X		

the only steel generally to be used for the single plate framing connection, the usefulness of information for the Grade 50 material warranted its inclusion in the test program.)

4. Plate thicknesses were varied by 1/16-in. from 1/4-in. plates to 5/8-in. plates.
5. Edge distances were 1 1/4 and 1 1/2 in. for 3/4-in. diameter bolts, 1 1/2 and 1 3/4 in. for 7/8-in. diameter bolts, and 1 3/4 and 2 in. for 1-in. diameter bolts.
6. Plate edges were sheared. Microcracks and fissures caused by shearing result in a more critical edge condition.
7. Bolt holes were punched (1/16-in. oversize).

Dimensions of the test plates are shown in Fig. 4. These dimensions of the plates were chosen to provide conditions similar to those around one bolt in a single plate framing connection.

The test plates were taken from the stock of and prepared by a local steel fabricator. All specimens were without any loose rust, with the mill scale left undisturbed. Tensile test coupons from the same stock as the test plates were ordered along with the test plates and were found to meet A36 and A572 Grade 50 specifications. The A325 and A490 bolts were also ordered from a local steel fabricator. No tests were run on the bolts; however, the bolts were taken from the fabricator's regular stock.

**Test Fixture for Single Shear Tests**—A test fixture, shown in Fig. 5, was designed for use in the 200,000 pound Tinius-Olsen screw type testing machine located in the Structures Laboratory at the University of Arizona. The fixture consisted of identical brackets, one bolted to the outside of the moving head and one to the fixed head. One-inch diameter hardened steel pins attached 1 3/8-in. x 3-in. connecting bars to the brackets. Two grips were each in turn pinned to the connecting bar by 1-in. pins. The test specimens were clamped into the grips by two 3/4-in. diameter A325 bolts. Shims were inserted between the test

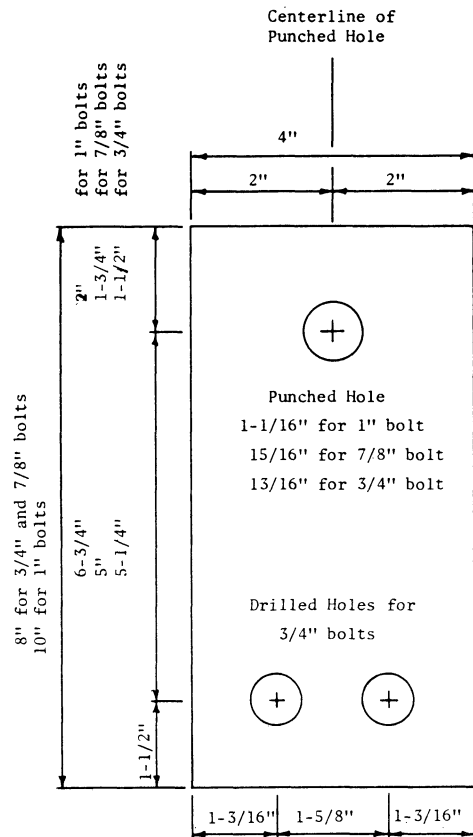


Fig. 4. Dimensions of test plates

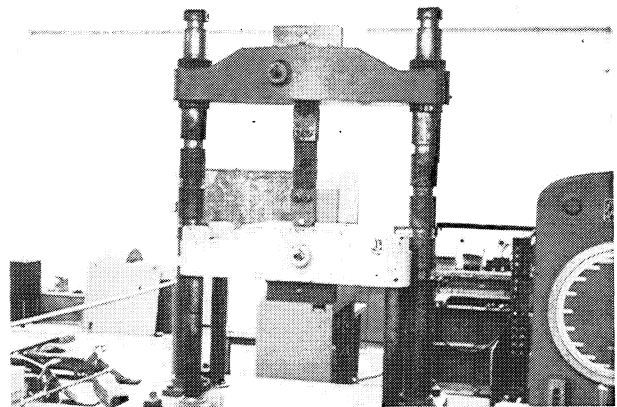


Fig. 5. Test fixture

plate and the grips to obtain the proper alignment of the specimens.

Deformations were measured by two dial gages, mounted to a bracket which was clamped to one of the test plates. A second bracket was clamped to the other test plate to provide benches for the probes of the dial gages. The use of two dial gages compensated for any out-of-plane bending that occurred in the test specimens.

**Test Procedure**—The test specimens were aligned in the test fixture and the bolts connecting the grips, shims, and test specimen were hand tightened. A preload of 5,000 lbs was then applied to the specimen to bring the bolt into bearing and to eliminate all slip from the connection. The connecting bolt was then tightened by the turn-of-the-nut method with the preload maintained. The preload was then removed and the dial gages were mounted. A load was then applied at a slow rate, with load and deformation readings taken at appropriate intervals.

**Load-Deformation Curves**—Tabulated results of the single bolt, single shear tests were obtained by averaging the dial gage readings and subtracting the elastic response of the connected plates. A plot of these data is given in Fig. 6. Superimposed on this plot is the curve representing a weighted least squares fit of the Richard formula.<sup>7</sup>

$$R = \frac{K_1 \Delta}{\left[ 1 + \left| \frac{K_1 \Delta}{R_0} \right|^n \right]^{1/n}} + K_p \Delta$$

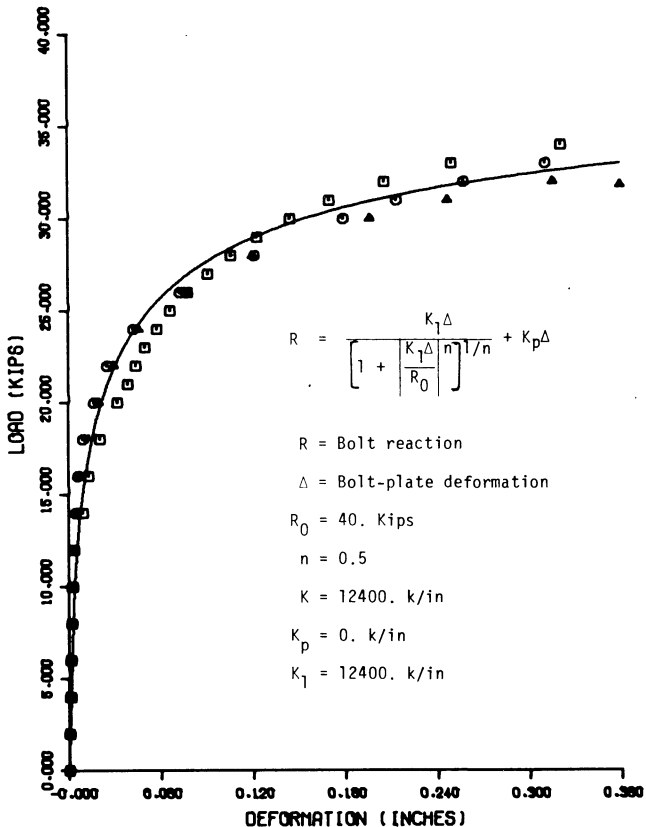


Fig. 6. Plot of load-deformation data for a  $3/4$ -in. diameter A325 bolt connecting two  $3/8$ -in. thick A36 plates

where

$R$  = bolt load

$\Delta$  = bolt-plate deformation

$R_0$  = bolt reference load

$n$  = bolt load-deformation curve shape parameter and with  $K_1$  and  $K_p$  defined as follows:

$K_p$  = slope of the load-deformation curve in the extreme yielding range

$K_1 = K - K_p$ , where  $K$  is the initial slope of the load-deformation curve

Table 2 gives the curve parameters for the single bolt, single shear tests for the specimens with edge distances given in Fig. 4.

The initial slope,  $K$ , of the load-deformation curve was determined by the formula:

$$K = 2E \frac{t_1 t_2}{t_1 + t_2}$$

where

$E$  = modulus of elasticity (29,000 ksi for steel)

$t_1, t_2$  = plate thicknesses

This equation was developed by the senior author through studies of unpublished Chance Vought tests for single fastener lap joint stiffnesses. Table 2 lists the curve parameters for the other plate and bolt combinations tested for this research project.

Table 2. Curve Parameters

Bolt	Plates, in.	$K$	$K_p$	$R_0$	$n$
$3/4$ -in. $\phi$ A325	$1/4$ - $1/4$ (A36)	7250	10	20	1.0
	$5/16$ - $5/16$ (A36)	9063	-10	50	0.4
	$3/8$ - $3/8$ (A36)	10875	0	40	0.5
	$7/16$ - $7/16$ (A36)	12700	10	40	0.5
	$1/2$ - $1/2$ (A36)	14500	20	30	0.7
	$1/4$ - $3/8$ (A36)	8700	-30	30	0.6
	$1/4$ - $1/2$ (A36)	9667	-30	30	0.6
	$3/8$ - $1/2$ (A36)	12400	0	40	0.5
	$3/8$ - $3/8$ (A572 Gr 50)	10875	20	30	0.7
$7/8$ -in. $\phi$ A325	$5/16$ - $5/16$ (A36)	9063	9	30	0.7
	$3/8$ - $3/8$ (A36)	10875	20	40	0.5
	$7/16$ - $7/16$ (A36)	12700	0	50	0.5
	$1/2$ - $1/2$ (A36)	14500	10	40	0.7
	$1/4$ - $3/8$ (A36)	8700	20	30	0.8
	$1/4$ - $1/2$ (A36)	9667	20	30	1.1
1-in. $\phi$ A325	$3/8$ - $1/2$ (A36)	12400	10	40	0.6
	$3/8$ - $3/8$ (A572 Gr 50)	10875	10	40	0.6
	$1/2$ - $1/2$ (A36)	14500	20	50	0.5
$3/4$ -in. $\phi$ A490	$5/8$ - $5/8$ (A36)	18125	0	90	0.4
	$1/2$ - $1/2$ (A36)	14500	-10	70	0.4
$3/4$ -in. $\phi$ A490	$3/8$ - $3/8$ (A36)	10875	0	40	0.6
	$7/16$ - $7/16$ (A36)	12688	0	60	0.4
	$5/8$ - $5/8$ (A36)	18125	10	60	0.4
	$1/2$ - $1/2$ (A36)	14500	40	40	0.7
	$5/8$ - $5/8$ (A36)	18125	40	50	0.5
$7/8$ -in. $\phi$ A490	$7/16$ - $7/16$ (A36)	12688	0	60	0.5
	$1/2$ - $1/2$ (A572 Gr 50)	14500	40	50	0.6
	$5/8$ - $5/8$ (A36)	18125	30	50	0.7
	$1/2$ - $1/2$ (A36)	14500	40	50	0.5
1-in. $\phi$ A490	$5/8$ - $5/8$ (A36)	18125	20	70	0.5
	$1/2$ - $1/2$ (A36)	14500	40	50	0.5

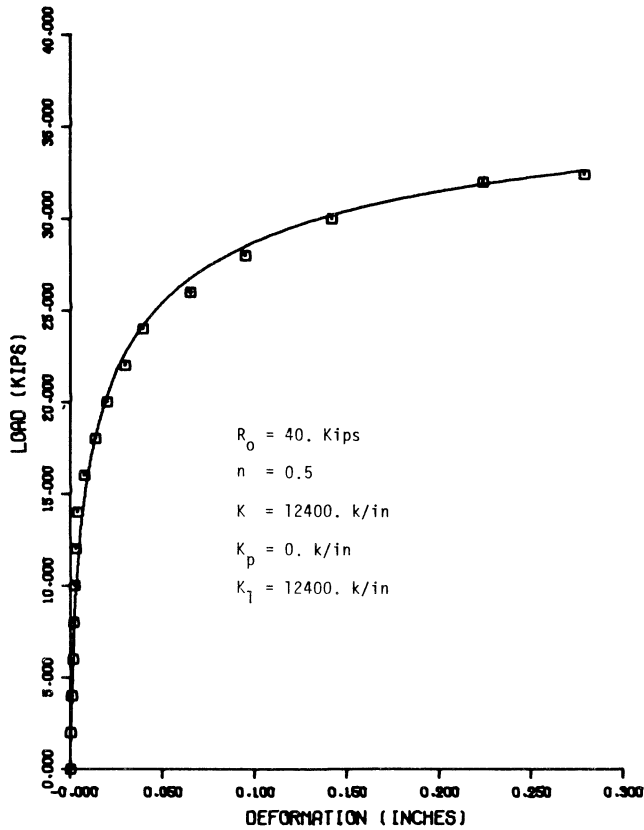
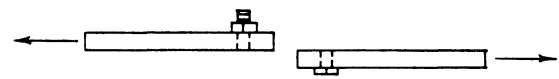


Fig. 7. Plot of load-deformation data for a  $3/4$ -in. diameter A325 bolt connecting  $3/8$ -in. and  $1/2$ -in. thick A36 plates

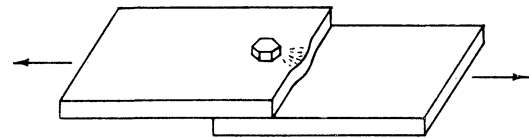
Figure 7 is the plot of the analytical expression for a  $3/4$ -in. diameter A325 bolt connecting one  $3/8$ -in. thick plate with second plate thickness of  $1/2$ -in. Similar plots were obtained for other plate thicknesses, as well as with varying bolt diameters. The important feature of this figure is that this curve does not vary significantly from that for Fig. 6, which indicates that the thinner plate in the combination will govern the load-deformation relationship. This is significant in that the framing plate and beam web thicknesses in single plate framing connections will generally not be the same; however, the strength and ductility of the connection will depend upon the characteristics of the thinner element.

**Failure Deformations and Modes**—Gaylord and Gaylord<sup>9</sup> list possible modes of failure that can occur in single shear connections. A description of these failure modes that were encountered in the single bolt, single shear tests were:

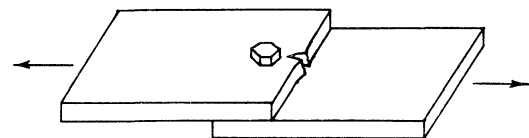
1. Shear failure of the bolt as shown in Fig. 8. This would be the most critical case since the connection is no longer capable of carrying any load.



Shear Failure of the Bolt



Bearing Failure of the Plate



Transverse Tension Tearing of the Plate

Fig. 8. Plate-bolt failure modes

2. Bearing failure of the plates in which yielding of the plate material takes place behind the bolt, as shown in Fig. 8. This case is not as critical, because the connection does not generally lose any load-carrying capacity.
3. Transverse tension tearing of the plate wherein a crack develops on the free edge and progresses toward the bolt, as shown in Fig. 8. This failure mode results in "strain softening" since the connection still has load-carrying capability, although at a reduced level.

In order to insure that the framing connection has ductility at the bolt line by circumventing the bolt shear and tension tearing modes of failure, it is recommended that: (a) the  $D/t$  ratios given in Table 3 or 4 be used for A36 beams and plates, and (b) an  $e/D$  ratio of 2.0 (see Fig. 4) should be provided. When these two modes of failure are circumvented, the bearing mode of failure occurs with the resulting desired ductile behavior. A deformation of 0.30 in. was used as the criterion for ductility in all the 48 single shear tests that were run to establish these criteria. This deformation would be about 1.25 times that required in the

**Table 3. D/t Ratios**

Bolt Size, in.	Web or Plate Thickness in Inches								
	1/4	5/16	3/8	7/16	1/2	9/16	5/8	11/16	3/4
3/4	3.0	2.4	2.0	1.71	1.5	1.33	1.20	1.09	1.00
7/8	3.5	2.8	2.33	2.0	1.75	1.56	1.40	1.27	1.17
1	4.0	3.2	2.67	2.29	2.0	1.78	1.60	1.45	1.33

|----- Limits—A325's -----> |  
 |----- Limits—A490's -----> |

**Table 4. Maximum Web or Plate Thickness, in.**

Bolt Size, ft	A325	A490
3/4	3/8	1/2
7/8	7/16	5/8
1	9/16	11/16

extreme bolts of an eleven-bolt connection in a W36 beam that has a 60-ft span and is uniformly loaded to 1.5 times its service load; that is,

$$\phi_{simple} \approx \frac{2 F_y L}{3 E d} = \frac{2(36)}{3(30 \times 10^3)} \frac{60 \times 12}{36} = 0.016 \text{ in.}$$

$$\Delta_{top \text{ bolt}} \approx \phi_{simple} \times \frac{h}{2} = 0.016 \times \frac{30}{2} = 0.240 \text{ in.}$$

where  $h$  is the depth of the bolt pattern. Figures 9 and 10 show typical transverse tearing and bearing failures, respectively, of test specimens with a deformation of 0.30 in.

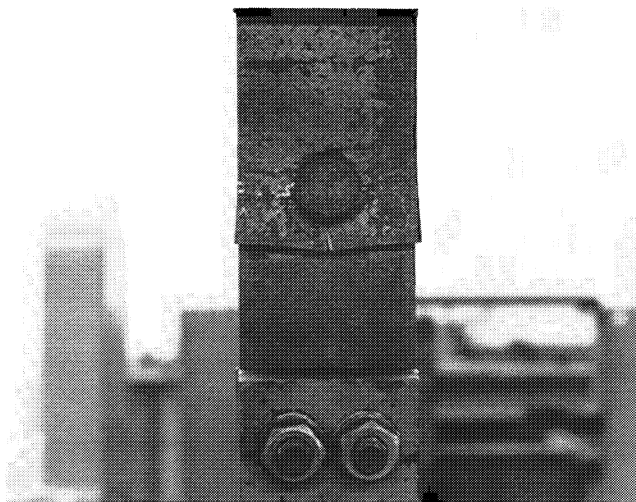


*Fig. 9. Transverse tension tear in test specimen*

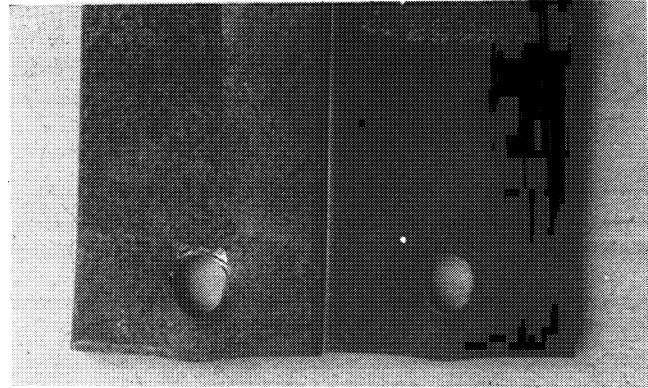


*Fig. 10. Bearing failure in test specimen*

**FINITE ELEMENT MODELS**

The procedure used for developing an appropriate finite element model capable of predicting the behavior of the single plate framing connection consisted of first creating a model that included the entire framing plate, bolts, and supported beam as shown in Fig. 11. Loads corresponding to those used by Lipson<sup>1</sup> in his tests were then applied to this model and results obtained were then compared to actual test results for verification. With the full beam and connection model thus verified, results were then obtained for a variety of loading conditions to determine patterns in the behavior of the connection. Based on these studies, simplified finite element models were then created which adequately predicted the connection behavior, but at a significant savings of effort and computer time.

**Program INELAS**—Program INELAS is a finite element program written to analyze plates stressed into the inelastic range and was the program used for the computer analysis.<sup>8</sup> The nonlinear structural response is calculated by a numerical algorithm that uses the Von Mises yield criterion and the associated flow rule.<sup>10</sup> Nonlinear uniaxial stress-strain relationships are represented in the INELAS program by the Richard equation.<sup>7</sup>

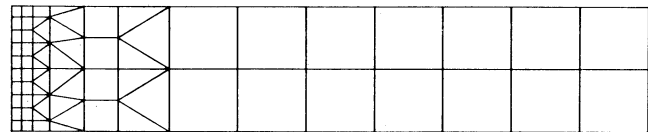


*Fig. 11. Finite element grid for full beam and connection model*

**Definition of Eccentricity**—The dimension in the single plate framing connection from the bolts line to the weldment at the supporting member is usually about 3 in., but can vary. Therefore, the eccentricity of the connection was defined as the distance from the bolt line to the point of inflection in the beam.

A nondimensional design parameter,  $e/h$ , is also defined here as the quotient of the eccentricity and the height of the bolt line as shown in Fig. 12.

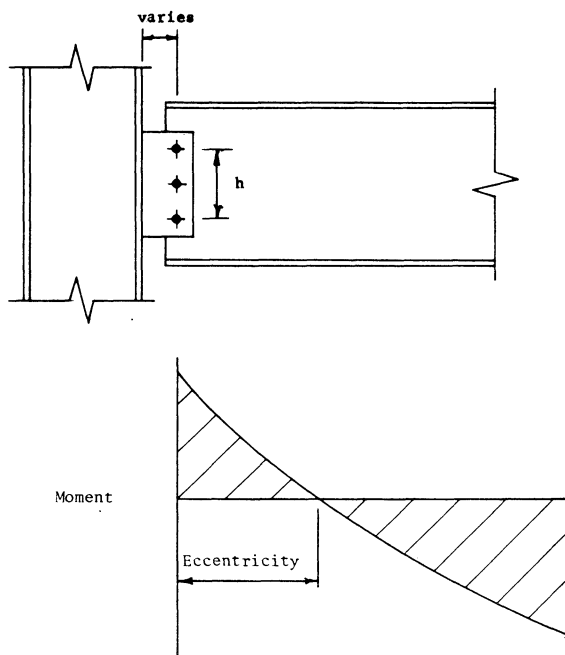


Fig. 12. Definition of eccentricity

**Numerical Studies of Behavior of the Connection**—The behavior of connections consisting of three to seven bolts were investigated for a variety of loading conditions. Finite element grids similar to that shown in Fig. 11 were used. From the results of these analyses, several important observations were made, as follows:

1. Virtually all the ductility of the connection is due to the deformation of the bolt and distortion of the plate around the bolt hole.
2. Under low loads, the outer bolt forces are nearly horizontal and give rise to the connection moment, whereas the inner bolt forces are nearly vertical and carry the connection shear. As the load is increased, the inelastic response of the connection causes the outer bolt force resultants to rotate toward a more vertical position, thereby carrying a larger portion of the connection shear. This action results in a reduction in the connec-

Table 5. Bolt Force Orientation for the Five-Bolt Test ( $L/d = 14$ ) in Degrees from Horizontal

Load, kips	No. of Bolts				
	1	2	3	4	5
8	0	13	90	167	180
16	1	11	90	169	179
24	2	10	90	170	178
32	4	11	90	169	176
40	5	13	90	167	175

Table 6. Bolt Forces in Kips for the Five-Bolt Test ( $L/d = 14$ )

Load, kips	No. of Bolts				
	1	2	3	4	5
8	9.8	5.1	1.7	5.1	9.8
16	16.0	10.6	3.6	10.6	16.0
24	19.2	15.0	5.7	15.0	19.2
32	20.6	17.7	8.3	17.7	20.6
40	21.5	19.3	11.1	19.3	21.5

tion eccentricity; however, the moment increases because of the increase in connection shear. Other researchers have noted this same action in the study of framed connections and observed from test specimens that the bolt holes were deformed and scored in a circular fashion.<sup>11</sup> Tables 5 and 6 give data obtained from Program INELAS in the analysis of the five-bolt test beam which illustrates these points. In these tables, bolts number 1 and 5 are the outer bolts, 3 is the center bolt, and 2 and 4 are the intermediate bolts.

3. The outer bolts are loaded to near their maximum capacity at loads well under the design service loading of the beam. Adding more bolts makes the connection stiffer, increases the eccentricity, and generally causes the outer bolts to reach their maximum capacity at even a lower beam load.

Moment rotation curves for two-, three-, five-, and seven-bolt framing connections were obtained by modeling cantilever beams with length  $e$ . These analyses showed that the moment-rotation curve was dependent upon the shear at the connection, as illustrated typically in Fig. 13, if  $e$  was less than  $h$ , where  $h$  is equal to the height of the bolt pattern. For  $e$  equal to or greater than  $h$ , the moment rotation relationship was insensitive to the connection shear. The results of these numerical studies were then used to derive the single nondimensional moment-rotation curve shown in Fig. 14. In this figure, the data points used to generate the original moment-rotation curves are shown as symbols. The middle curve is the plot of the nondimensional equation. The upper and lower curves represent the range in which data falls within ten percent of the nondimensional equation.

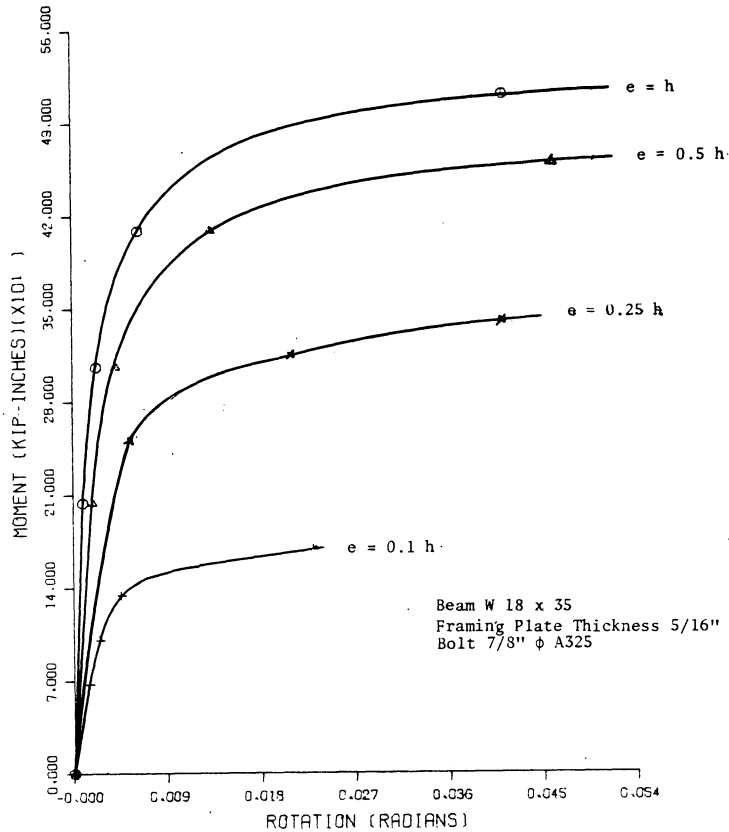


Fig. 13. Moment-rotation relationship for five-bolt connection

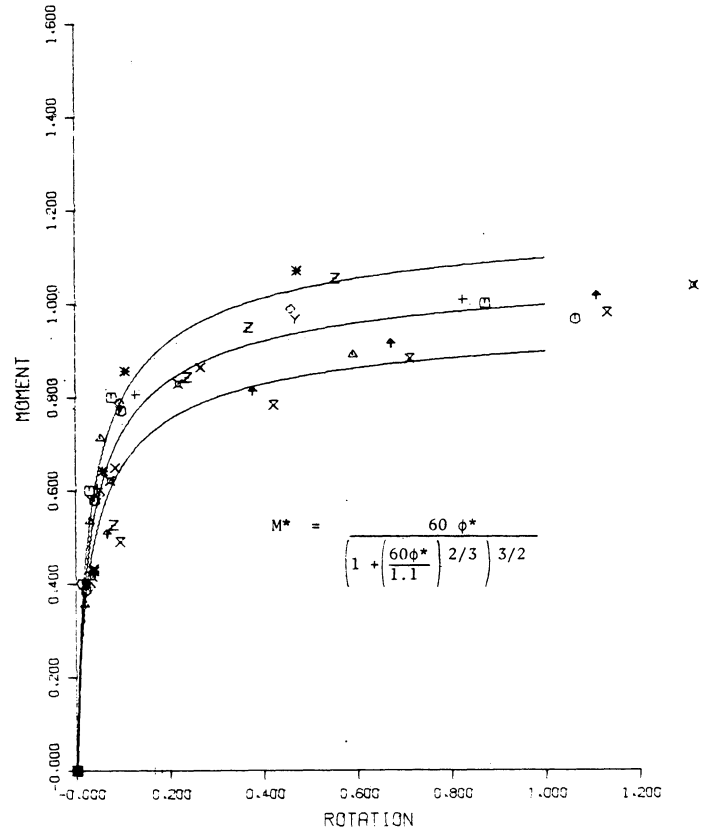


Fig. 14. Nondimensional equation with 10% bounds superimposed on reduced moment-rotation curve data points

In summary, this equation is constructed as follows:

$$M^* = \frac{60 \phi^*}{\left[1 + \left(\frac{60 \phi^*}{1.1}\right)^{2/3}\right]^{3/2}}$$

and

$$M = M^* [1 - (1 - e/h)^{3.9}] M_{ref}$$

where

- $M$  = moment in the connection
- $M_{ref}$  = reference moment based on a pure moment being applied to a connection and all bolts being loaded to their maximum capacities
- $M^*$  = intermediate nondimensional moment value
- $\phi^*$  = free end rotation of the beam divided by a reference rotation value  $\phi_{ref}$

$$\phi_{ref} = \frac{0.3 \text{ in.}}{\left[\frac{(n-1)(3 \text{ in.})}{2}\right]}$$

- $n$  = number of bolts
- $e$  = eccentricity of the load
- $h$  = depth of the bolt pattern

Tables 7 and 8 summarize the data required for the use of the above equations based on data obtained through use of the results of the single bolt, single shear tests for A36 steel plates.

This equation was then used to numerically model experimental results obtained by Lipson for the pure moment case. A comparison of the analytical and experimental results is shown in Fig. 15, where the two sets of experimental data for each connection essentially envelope the analytical curve.

Table 7.  $\phi_{ref}$  for Use in the Nondimensional Moment-Rotation Equation

No. of Bolts	$\phi_{ref}$ (radians)
3	0.1
5	0.05
7	0.0333
9	0.025

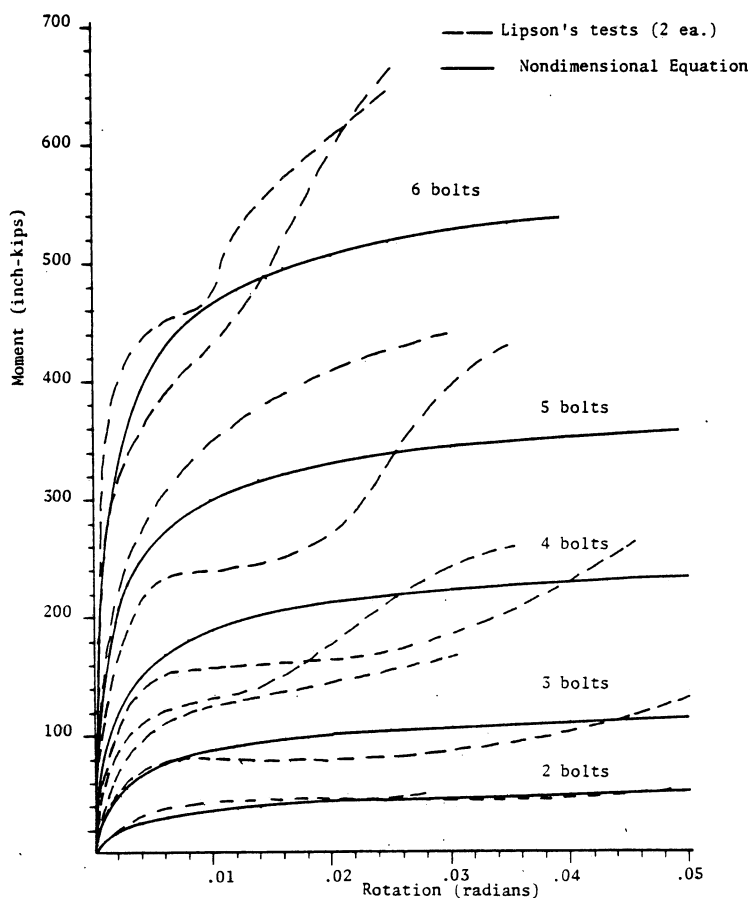


Fig. 15. Lipson's test results with predictions by nondimensional equation superimposed

### EXPERIMENTAL MOMENT-ROTATION CURVES

A total of seven tests were made using the test fixture shown in Fig. 16. The two-, three-, five-, and seven-bolt tests were run with the framing connection plate welded to a flange plate which was in turn bolted to the support column. A second set of tests was run on the two-, three-, and five-bolt connections with the framing connection plate welded to the support column. In both sets of tests the rotation was measured by the rotation bars giving beam-to-plate rotation, as shown in Fig. 17, and by dial gages mounted on the top and bottom flanges of the test beam giving beam to column rotation. In all tests the beam length was equal to the depth of the bolt pattern ( $e/h = 1$ ). Figure 18 gives the

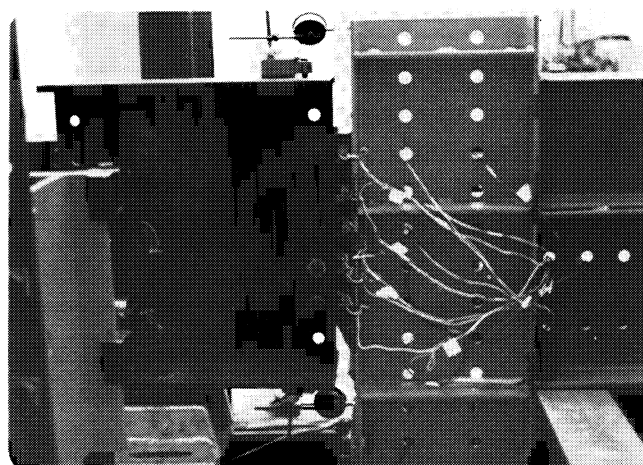


Fig. 16. Experimental moment-rotation test configuration

Table 8.  $M_{ref}$  Values in Kip-In., Based on Test Results for Use in the Nondimensional Moment-Rotation Equation

3/4-in. Diam. A325 Bolts				
Minimum Plate Thickness, in.	No. of Bolts			
	3	5	7	9
1/4	120	358	716	1194
5/16	146	437	875	1458
3/8	200	600	1200	1998
7/16	210	628	1256	2094
1/2	200	594	1188	1980
7/8-in. Diam. A325 Bolts				
1/4	138	420	836	1393
5/16	169	506	1012	1686
3/8	234	702	1404	2340
7/16	239	718	1436	2394
1/2	233	698	1397	2328

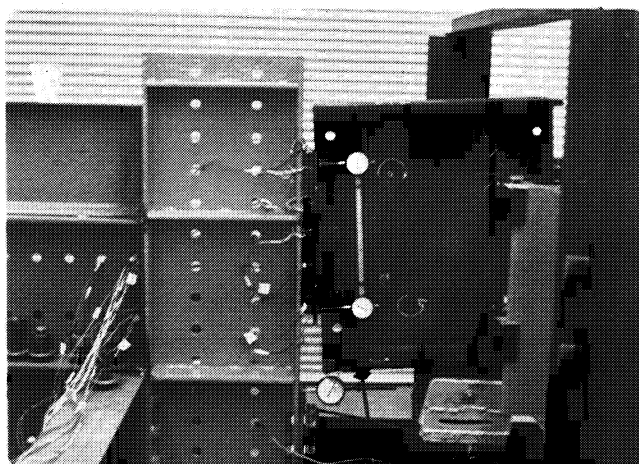


Fig. 17. Rotation bars

moment-rotation curves for the two-bolt connection, as well as the analytically predicted curve. Similar information is given in Figs. 19 and 20 for the three- and five-bolt connections, respectively. Figure 21 gives the moment-rotation curve for the seven-bolt connection in which the framing plate was welded to a flange plate bolted to the supporting column. Figure 22 summarizes the test results by giving the moment rotation curves for the two-, three-, five-, and seven-bolt tests in nondimensional form along with the nondimensional analytical curve with  $\pm 10\%$  bounds.

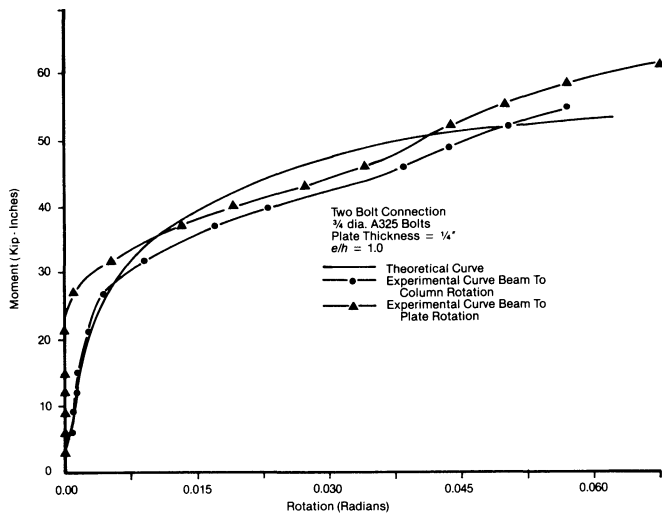


Fig. 18. Moment-rotation curve—two bolt single plate framing connection (welded)

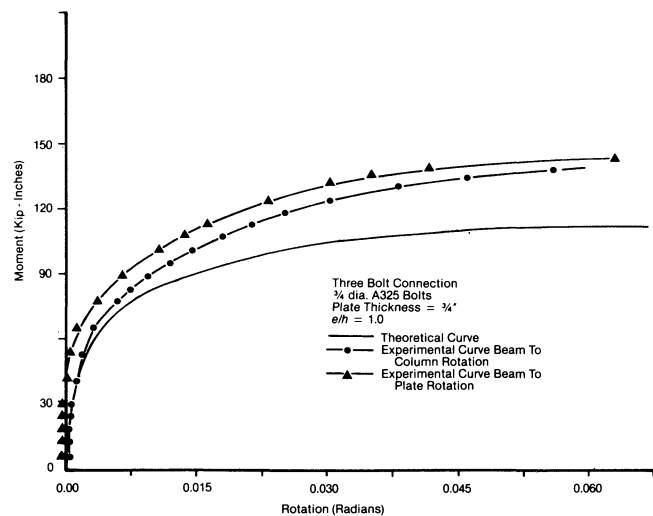


Fig. 19. Moment-rotation curve—three bolt single plate framing connection (welded)

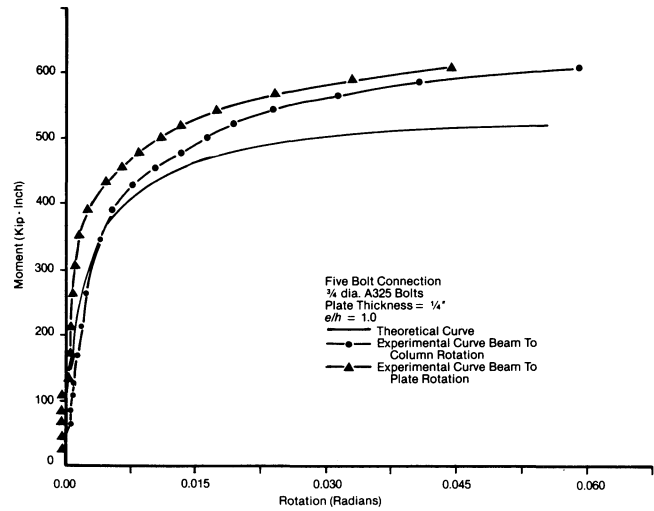


Fig. 20. Moment-rotation curve—five bolt single plate framing connection (welded)

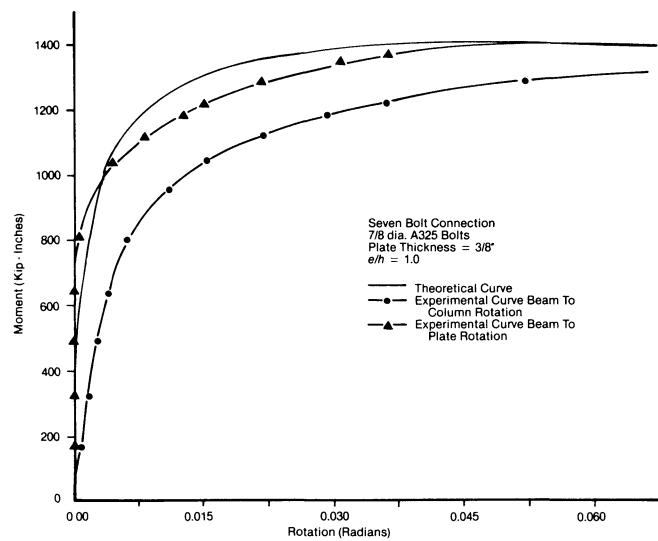


Fig. 21. Moment-rotation curve—seven bolt single plate framing connection (bolted)

### FULL SCALE BEAM TESTS

Five full scale beam tests were scheduled, as shown in Table 9. The framing plates and beams had  $1\frac{1}{2}$ -in. and  $1\frac{7}{8}$ -in. edge distances for the  $\frac{3}{4}$ -in. and  $\frac{7}{8}$ -in. bolts, respectively, with punched holes 3 in. on center. Using the test configuration shown in Fig. 23, the eccentricity as a function of the applied load was measured by means of the strain gages located on the top and bottom flanges of the beam between the load and the connection, and also by computing the connection moment from the beam reaction.

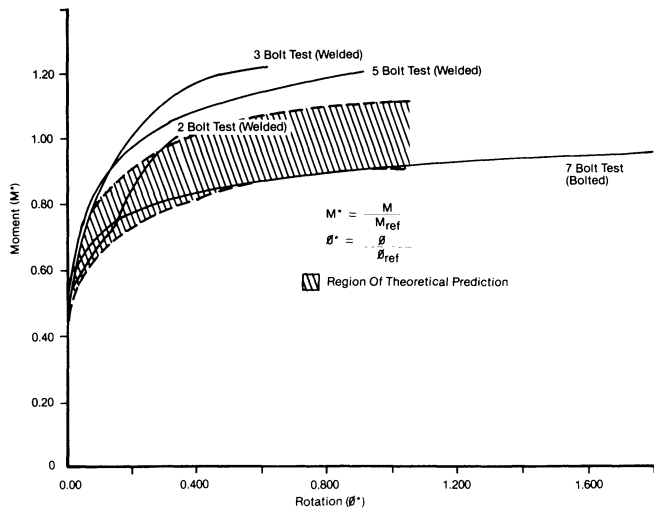


Fig. 22. Nondimensional moment-rotation curves

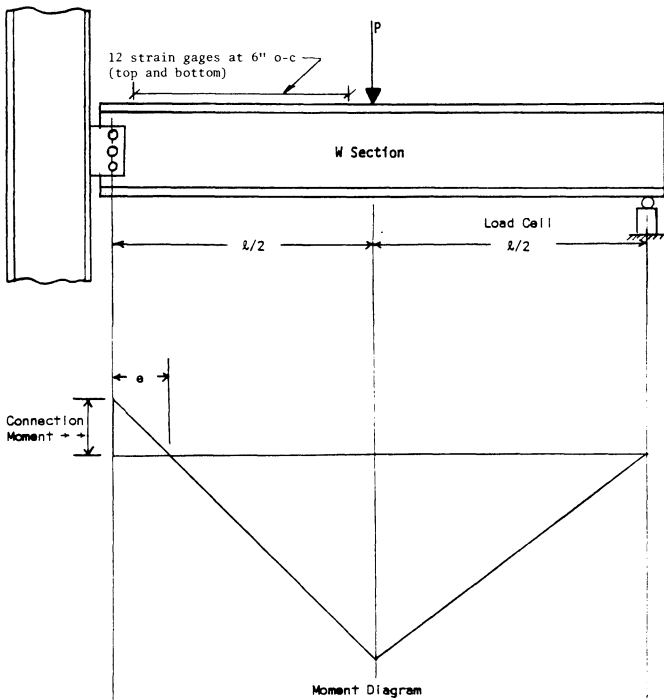


Fig. 23. Test configuration

Table 9. Full Scale Beam Test Schedule

Beams (A36)	L/D	Framing Plates (A36), in.	Bolts (A325)	
			No.	Diam., in.
W18 × 35 $t_{web} = 0.300$ in.	14	5/16	3	3/4
	14	5/16	5	3/4
	8.9	5/16	5	3/4
W24 × 55 $t_{web} = 0.394$ in.	16	3/8	7	7/8
	16	3/8	3*	7/8

\* Bolt pitch = 6 in.

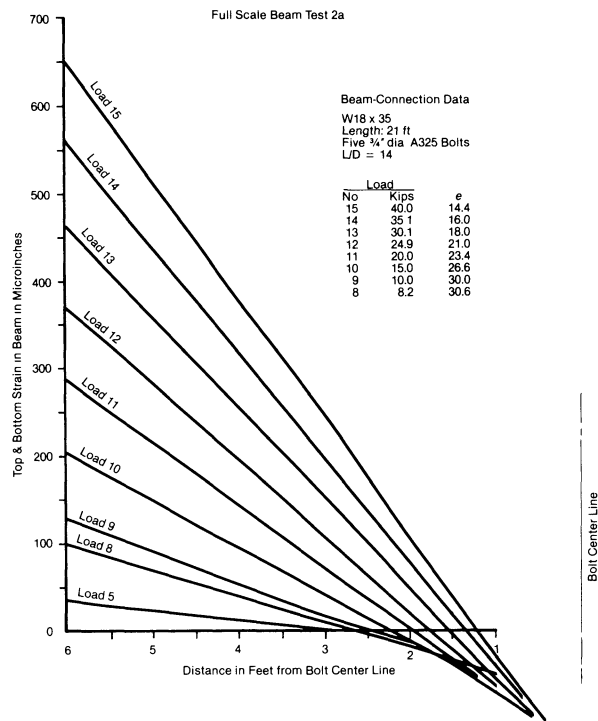


Fig. 24. Five bolt test strain data

Table 10. Connection Eccentricities—Analytical and Experimental Results

Beams	Bolts (A325)	L/D	Connection Eccentricity, in.			
			Program INELAS	Beam Line Theory	Design Curve Prediction	Full Scale Test
W18×35	3 — 3/4 in.	14	5.9	5.8	6.2	4
W18×35	5 — 3/4 in.	14	15.6	18.7	20.6	14.4
	5 — 3/4 in.	8.9	11.9	12.3	11.5	12.7
W24×55	7 — 7/8 in.	16	43.3	48.0	49.5	42.2
	3 — 7/8 in.	16	15.8	17.3	14.2	19.3

**Table 11. Measured vs. Predicted Eccentricity for the Five-Bolt Connection with  $L/d = 14$**

Applied Load $P$ , kips	Connection Moment, kip-in.	Eccentricity, $e$ , in.	
		Predicted by Beam Line Theory	Measured
4.0	105	43.3	33.8
15.0	280	32.4	26.6
30.0	375	22.7	18.0
35.0	390	20.4	16.0
40.0	405	18.7	14.4

**Three-Bolt Test Results**—The three-bolt test results for the W18 × 35 beam are given in the first line of Table 10, along with the computed results for a central load of 40 kips and a beam length of 20.6 ft. This load causes a maximum bending stress of 40.4 ksi based upon linear beam stress theory. When the beam was unloaded, a very small amount of permanent deflection remained. When the beam was disconnected from the framing plate, neither the bolts nor the beam web or plate showed any measurable distortion or distress. This could be expected since only a distortion of 0.025 in. in the outer bolts is required to accommodate a simple beam end rotation for this three-bolt connection.

**Five-Bolt Test Results**—The test configuration for the first five-bolt test was identical to the three-bolt test. Results from this test are given in Fig. 24 and in Tables 10 and 11, where beam strains and connection eccentricities are given as a function of the load, respectively. As with the three-bolt test, no measurable distortion or distress was observed in the connection elements when the beam was disconnected from the framing plate.

The test configuration for the second five-bolt test was similar to the first, except that the beam length was reduced to 13.33 ft to give an  $L/d$  equal to 8.9. Strain and load cell data were taken at appropriate intervals up to a load of 55.0 kips, which caused a maximum bending stress of 36 ksi and is 1.5 times the working stress allowable for this beam.

The measured eccentricity which was found from the measured strain data and also computed from the beam reactions is given in Table 10 for this 55.0 kip load. This beam was then loaded to 80.5 kips, which caused yielding in the beam under the concentrated load. Upon loading a permanent center line deflection of approximately 1/2-in. remained in the beam. Using plastic analysis, a stress of 44 ksi was computed for this 80.5 kip load. When the beam was disconnected from the framing plate, some hole distortion was observed, indicating the desired ductile behavior had occurred.

**Seven-Bolt Test Results**—The seven-bolt test results for the W24 × 55 beam are also given in Table 10. These analytical and experimental results demonstrate that very

significant moment can result when deep bolt patterns are used. The connection moment for the 42 kip load (which is 1.5 times the working load for this beam) is 1150 kip-in. This moment is thirty-seven percent (37%) of the fixed end moment. When the beam was disconnected from the plate, neither the bolts nor the plate and beam web showed any significant distortion or distress.

**Three-Bolt Test with Six-Inch Bolt Pitch**—This test was run to demonstrate the independence of bolt pitch in the design formulas and also to observe experimentally the performance of such a bolt pattern in this connection. The eccentricities as determined analytically and experimentally for the 42 kip central load are given in Table 10. When the beam was unbolted from the connection plate, some hole distortion was observed, indicating the effect of increasing the bolt pitch.

**Test Summaries**—Table 10 summarizes the analytical and experimental test results giving the values of the connection eccentricity as obtained by: (a) the full finite element model using Program INELAS, (b) beam line theory using the nondimensional moment rotation curve developed in this research effort, (c) the design curve and formulas which include an adjustment to account for the concentrated load, and (d) the experimental tests. The agreement of the predicted and measured eccentricities was very satisfactory. All beams were loaded to at least 1.5 times the working load, and in all cases the connections performed satisfactorily by exhibiting no significant distortion or distress.

**Table 12. Beam and Bolt Schedule for Design Curves**

Beam	Section Modulus, in. <sup>3</sup>	Bolt Diam., in.
W14× 22	29.0	3/4
W16× 26	38.3	3/4
W16× 40	64.6	3/4
W18× 35	57.9	3/4
W18× 55	98.4	3/4
W21× 44	81.6	3/4
W18× 55	98.4	7/8
W21× 44	81.6	7/8
W21× 68	140.0	7/8
W24× 76	176.0	7/8
W24× 84	197.0	7/8
W24× 94	221.0	7/8
W27× 94	243.0	7/8
W24× 94	221.0	1
W27× 94	243.0	1
W30×116	329.0	1
W33×118	359.0	1
W33×141	448.0	1
W36×135	440.0	1
W36×182	662.0	1

## DESIGN FORMULAS

In order to facilitate the design of the plate and weldment using nondimensional moment-rotation curves and beam line theory, an extensive multidimensional parameter search was made to develop design aids. The results of this study, which used the beam and bolt schedule given in Table 12 and about 1500 beam line analyses, are presented in Fig. 25, where a weighted least squares design curve with  $\pm 20\%$  bounds is also given. This curve, which is for beams with uniform load, yields a parameter called  $(e/h)_{ref}$  based upon the beam  $L/d$  ratio. The  $e/h$  of a given connection is then computed as follows:

$$e/h = (e/h)_{ref} \times \left(\frac{n}{N}\right) \times \left(\frac{S_{ref}}{S}\right)^{0.4}$$

where

$n$  = number of bolts

$N$  = 5 for  $3/4$ -in. and  $7/8$ -in. bolts, and 7 for 1-in. bolts

$S_{ref}$  = 100 for  $3/4$ -in. bolts, 175 for  $7/8$ -in. bolts, and 450 for 1-in. bolts

$S$  = section modulus of beam

This design curve is independent of bolt pitch. To use this design aid for concentrated loads, multiply the value of  $e$  obtained for uniform load case by the eccentricity coefficients given in Appendix A.

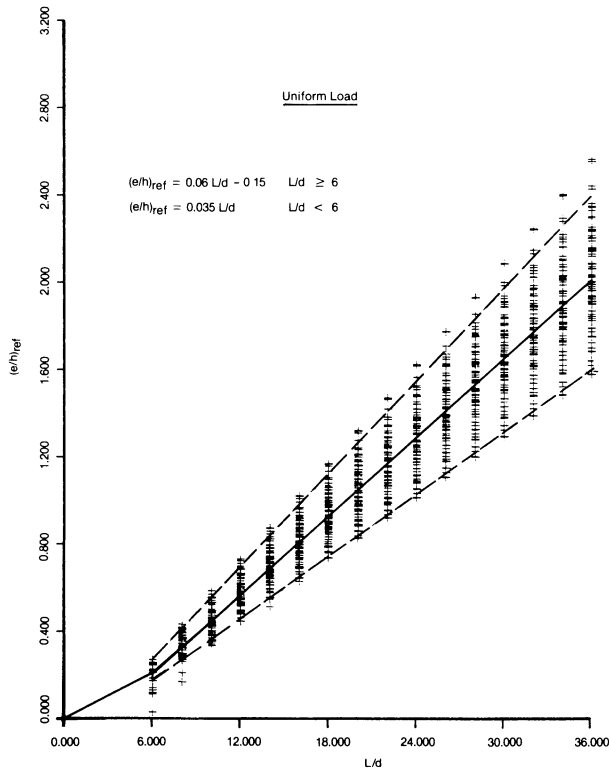


Fig. 25. Design curve with  $\pm 20\%$  bounds

## RECOMMENDED DESIGN PROCEDURE

Listed below is a detailed design procedure that is based upon the results of the analytical and experimental research study on single plate framing connections.

1. Select plate thickness  $\pm 1/16$ -in. of supported beam.
2. Compute number of bolts required based upon allowable beam shear and allowable bolt loads. Insure connection ductility by providing: (a) the bolt diameter to plate (or beam web) thickness ratio according to Table 5, and (b) a plate edge to bolt diameter ratio of two.
3. Enter the design curve with the beam  $L/d$  ratio and read  $(e/h)_{ref}$ . Use the design formulas to calculate  $e/h$  for the connection. Compute  $h$ :

$$h = (n - 1) \times p$$

where

$n$  = number of bolts

$p$  = pitch

With the ratio  $e/h$  and  $h$  known, compute the connection eccentricity,  $e$ .

4. Compute the moment at the weldment:

$$M = V \times (e + a)$$

where

$V$  = beam shear force

$e$  = eccentricity from step 3

$a$  = distance from the bolt line to the weldment

5. Check the plate normal and shear stresses:

$$f_b = \frac{M}{1/4 t b^2}$$

$$f_v = \frac{V}{b t}$$

where  $t$  and  $b$  are the plate thickness and depth, respectively.

6. Design the weldment based upon the resultant of the normal and shear stresses from step 5:

$$f_r = (f_b^2 + f_v^2)^{0.5}$$

### Remarks on the Design Procedure

1. If according to step 6 a thinner plate will be adequate, such plate may be selected. Use A36 material.
2. The number of bolts computed here assumes equal shear in each bolt. This research has shown that this is not true; however, by designing ductility into the connection through the prevention of bolt shear and tension tearing, adequate redistribution of the shear in the bolt pattern results in satisfactory connection performance at the bolt line.

3. The design curves are independent of the bolt pitch.
4. The distance from the bolt line to the weldment line, denoted here as  $a$ , is usually about 3 in.
5. The formula used to compute the normal plate stress is not a consequence of plastic plate action, but results from the fact that all outer bolts of the connection have force resultants that are nearly equal and horizontal (i.e., normal to the bolt line).

#### ACKNOWLEDGMENT

The Committee of Structural Steel Producers and the Committee of Steel Plate Producers of the American Iron and Steel Institute funded this research. The Task Force of Projects 302 and 305, chaired by Mr. Ernest D. Hunter, monitored this study. The authors extend their appreciation to the members of this group for their help and guidance.

#### REFERENCES

1. Lipson, S. L. Single-Angle and Single-Plate Beam Framing Connections *Proceedings, Canadian Structural Engineering Conference, Toronto, Ontario, Canada, Feb. 1968, pp. 141-162.*
2. Lipson, S. L. Single-Angle Welded-Bolted Connections *Journal of the Structural Division, ASCE, Vol. 103, No. ST3, Proc. Paper 12813, March 1977, pp. 559-570.*
3. Caccavale, S. E. Ductility of Single Plate Framing Connections *Thesis presented to University of Arizona, at Tucson, Arizona, in 1975, in partial fulfillment of the requirements for the Master of Science degree.*
4. Batho, Cyril Second Report *Steel Structure Research Committee, Dept. of Scientific and Industrial Research of Great Britain, H. M. Stationery Office, London, 1934.*
5. Gillett, P. E. Ductility and Strength of Single Plate Connections *Dissertation presented to the University of Arizona, at Tucson, Arizona, in 1978, in partial fulfillment of the requirements for the degree of Doctor of Philosophy.*
6. Hectman, R. A. and B. G. Johnston *Riveted Semi-Rigid Beam-to-Column Building Connections Progress Report No. 1, Committee on Steel Structures Research, AISI, Nov. 1947.*
7. Richard, Ralph M. Versatile Elastic-Plastic Stress-Strain Formula *Journal of Engineering Mechanics Division, ASCE, Vol. 101, No. EM4, Proc. Paper 11474, Aug. 1975.*
8. Richard, Ralph M. User's Manual for Nonlinear Finite Element Analysis Program INELAS *Dept. of Civil Engineering, The University of Arizona, Tucson, Ariz., 1968.*
9. Gaylord, Edwin H., Jr. and Charles N. Gaylord *Design of Steel Structures Second Edition, McGraw-Hill, Inc., New York, N.Y., 1972.*
10. Richard, Ralph M. and James R. Blacklock *Finite Element Analysis of Inelastic Structures AIAA Journal, Vol. 7, No. 3, March 1969.*
11. Crawford, Sherwood F. and Geoffrey L. Kulak *Eccentrically Loaded Bolted Connections Journal of the Structural Division, ASCE, Vol. 103, No. ST3, Proc. Paper 7956, March 1971.*

#### APPENDIX A—ECCENTRICITY FOR CONCENTRATED LOADS USING THE UNIFORM LOAD DESIGN CURVE

In general, the eccentricity is:

$$e = \frac{M_{conn}}{V_{beam}} \quad (1)$$

When the beam is loaded to its first yield load, the  $M_{conn}$  vs  $\phi$  curve is essentially flat, so that  $M_{conn}$  may be considered independent of  $\phi$ . Let  $W_{FY}$  be the first yield uniform load. Then,

$$M_{beam} = \frac{1}{8} W_{FY} l = F_y S$$

so

$$\frac{W_{FY}}{2} = V_{beam} = \frac{4F_y S}{l}$$

and

$$e_{uniform} = \frac{M_{conn}}{4F_y S} \quad (2)$$

Similarly for a central load of  $P_{FY} = W_{FY}$ ,

$$M_{beam} = \frac{1}{4} W_{FY} l = F_y S$$

so

$$\frac{W_{FY}}{2} = V_{beam} = \frac{2F_y S}{l}$$

and

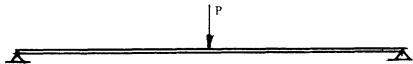
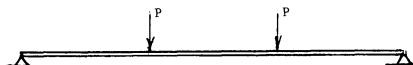
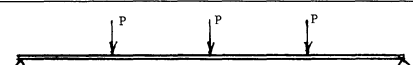
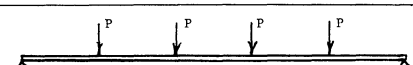
$$e_{conc} = \frac{M_{conn}}{2F_y S} \quad (3)$$

From Eqs. (2) and (3), the eccentricity coefficient is computed as follows:

$$\frac{e_{conc}}{e_{uniform}} = 2$$

In a similar manner, other loading cases may be treated as shown in Table 1A.

Table 1A. Eccentricity Coefficients for Concentrated Loads

Type of Loading: Equal Loads, Equal Spaces	Eccentricity Coefficient
	2.00
	1.33
	1.33
	1.20

APPENDIX B—DESIGN EXAMPLE

**Given:** W24 x 68, A36 steel,  $S = 153 \text{ in.}^3$   
 Span: 24 ft, laterally supported  
 Loading: Uniform with  $W = 102 \text{ kips}$

**Solution:**

1. Select  $t_{plate} = 3/8\text{-in.}$  ( $t_{web} = 0.416 \text{ in.}$ )
2. Try  $3/4\text{-in.}$  A325 bolts,  $R = 102/2 = 51 \text{ kips}$   
 $D/t = 3/4 \div 3/8 = 2$   
 $N_{req'd} = 51 \text{ kips} / 9.28 \text{ kips} = 6 \text{ bolts}$
3.  $(e/h)_{ref} = 0.06 \ 1/d - 0.15 = 0.57$   
 $(e/h) = 0.57 \times \left(\frac{6}{5}\right) \times \left(\frac{100}{153}\right)^{0.4} = 0.57$

With  $p = 3 \text{ in.}$ ,  $h = (6 - 1) \times 3 = 15 \text{ in.}$

$$e = 0.57 \times 15 = 8.55 \text{ in.}$$

4. For  $a = 3 \text{ in.}$ ,  $V = R = 51 \text{ kips}$   
 $M = 51 \times (8.55 + 3) = 589 \text{ kip-in.}$
5.  $f_b = \frac{4 \times 589}{0.375 \times 18^2} = 19.4 \text{ ksi} < 24 \text{ ksi}$   
 $f_v = \frac{51}{0.375 \times 18} = 7.56 \text{ ksi}$
6.  $f_r = (19.4^2 + 7.56^2)^{1/2} = 20.8 \text{ ksi}$   
 $70\text{XX weld req'd} = \frac{20.8 \times 0.375}{0.93} = 8.4 \text{ sixteenths}$

Use  $5/16\text{-in.}$  fillets each side.